

## **Dynamic Voltage Stability Analysis on Shore-to-Ship Power Connected System**

**Welma Nyabuto**

*Department of Electrical Engineering, Pan African University Institute of Basic Science, Technology and Innovation, Republic of Kenya*

**Christopher Maina**

*Department of Electrical Engineering, Murang'a University of Technology, Republic of Kenya*

**Peter Kihato**

*Department of Electrical Engineering, Jomo Kenyatta University of Agriculture and Technology, Republic of Kenya*

### **Abstract**

The shore to ship power connection is a technology that has been recommended as one of the ways that will help reduce emissions from marine vessels which have increased in number as a result of rapid growth in international trade. The interconnection of marine vessels at berth to an existing shore power grid has raised concerns to system operators and regulators regarding the system's stability because the on and off addition of loads to the network leads to fluctuations on the voltage stability of the system. This paper analyzes the dynamic voltage stability response of the Kenyan coastal power system interconnected to an off-shore load before and after the connection of automatic voltage regulators (AVR) under a three-phase fault. A static synchronous compensator (STATCOM) was introduced to assess its effectiveness before and after the ship load increase. The results showed that before the off-shore load increase, the AVRs are able to provide enough compensation to the ship motor loads. However, after increasing the load, the system experiences voltage collapse but the application of STATCOM in the system will help prevent voltage collapse.

**Keywords:** AVR, Dynamic Voltage Stability, Off-shore load, STATCOM, Three-phase fault

## **I. INTRODUCTION**

The increase in the number of ships at sea and berth has been found to have negative environmental impacts including air pollution. The emitted gases including nitrogen oxides (NO<sub>x</sub>), particulate matter (PM), Sulphur oxides (SO<sub>x</sub>), carbon oxide (CO) and carbon dioxide (CO<sub>2</sub>) not only causes serious danger to the natural environment but also to human health. To reduce this shipping related pollution, both local and international organizations such as International Maritime Organizations (IMO) have given recommendations on how to reduce these emissions. The proposed ways to reduce the shipping related pollution include usage of low Sulphur fuel, liquified natural gas as a fuel, scrubber's systems and shore connection systems. Shore to ship connection has been found to be the most effective way to reduce costs and minimize the pollution. The connection cuts all emissions, vibrations and noise associated with ships at berth. The onshore power connection involves the turning off of the diesel engines in commercial ships when berthing and tapping of power from the shore to meet their demands including lighting, ventilation, cooling, loading and offloading activities [1][2] [3].

The interconnection of the ships to the shore network grid presents some challenges on the stability of the power network. The onboard loads are on and off and this intermittent nature shows more variations and fluctuations on the actual load demand. These variations lead to oscillations that affect the voltage stability of the power network [4]. Power distribution in the onboard system of marine vessels is equivalent to a small-scale industrial power grid with a large percentage of the loads being represented by motors. The ship system is largely influenced by induction motors. During contingencies like a fault, induction motors draw more current from the system leading to a drop in the voltage profiles of the system. If enough reactive power compensation is not provided, extended draw of current from the system by the motors will lead to a complete voltage collapse resulting to a total or partial blackout [5].

Ion et al [5] performed an analysis on the behavior of the shore to ship power connected system under steady state and transient conditions. The focus was on the transients resulting from the behaviors of the induction motors of the ship system with limitation on the fault current that can be handle by the grid frequency converter (GFC). Simulation on the transient behavior of the induction motors was done and the effects during a short circuit scenario were investigated. It was established that during a fault, large fault current flows exceeding the limit set on the GFC system lead to unstable voltages. If the fault period exceeds the time threshold of the GFC's protections', it leads to a total blackout on the shore system. Karue et al [6] developed an aggregate load model for the ship loads and used it to analyze the impact on voltage stability by interconnecting the ship load to the on-shore grid. The study revealed that the model showed characteristics associated with induction motor loads. This aggregated model was connected to an existing land power grid and then used to assess the loading limit of the system. In the research [7], the continuation power flow approach was used to predict the breaking point of a shore to ship connected power system by increasing its load step by step. The study in [8] investigated voltage

stability on a 132kV line linked to ship loads. A continuation power flow analysis was performed and the loading limits of the system were determined.

Interconnected power networks are prone to faults and disturbances and these challenges lead to either an increase or decrease of power flow in the transmission network. The occurrence of disturbances on the system cause components like transmission lines and generators to trip subjecting the system to instability and cascading outages. Increased loading on the lines result to voltage collapse due to lack of enough reactive power compensation [9]. The dynamic assessment of the stability status of the power network is of significant value in preventing power outages. The occurrence of a disturbance leading to instability needs to be recognized fast and the necessary control measures be put into place.

In this paper, a dynamic model of the Kenyan coastal power network with the off-shore loads is developed using the PSAT MATLAB toolbox. Dynamic voltage stability analysis is done using the developed model before and after employing the automatic voltage regulators (AVRs) on the generators under a disturbance, 3-phase fault. In order to improve the system's stability, the static synchronous compensator (STATCOM) is introduced to assess its effectiveness during contingencies to avoid total or partial voltage collapse of the system before and after increasing the off-shore load.

## **II. METHODOLOGY**

### **II.I Grouping and aggregation of motor loads**

A power system network with many induction motors requires more time to successfully do a simulation due to its complexity. It is very crucial to obtain the right equivalent aggregate parameters for the induction motors since motors have a huge effect on the voltage stability of a power system. Different approaches have been used to obtain the aggregate parameters. These include a dynamic aggregation approach [10], transformer type equivalent circuit method and obtaining an equivalent induction motor circuit under two operating conditions, no-load and locked rotor as proposed in [11]. Karakas et al [12] and Kataoka et al [13] did further work and proposed an approach that is less tedious and can be used to obtain parameters of an aggregate equivalent circuit for a group of induction motors effectively.

The equivalent circuit aggregated model of induction motors where N stands for the number of motors is shown in Fig. 1. It is assumed that the motors are connected in parallel at the same bus and the supply voltage is the same.

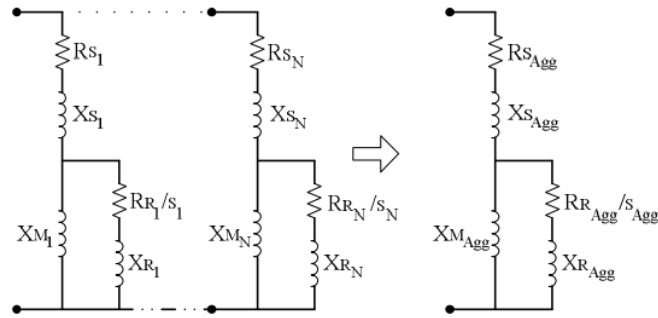


**Fig. 1.** Equivalent model of aggregated induction motor

$R_S$ ,  $X_S$ ,  $R_R$ ,  $X_R$ ,  $X_M$  and  $S$  denote stator resistance, stator reactance, rotor resistance, rotor reactance, magnetizing reactance and slip respectively.

In this paper, the following formulas were used to obtain the aggregated parameters of the ship motor loads [12]:

$$R_{S_{Agg}} = \text{real}(Z_{NLeq}) \tag{1}$$

$$R_{R_{Agg}} = \text{real}(Z_{LReq}) - \text{real}(Z_{NLeq}) \tag{2}$$

$$X_{sagg} = \frac{n}{n+1} \cdot \text{imag}(Z_{LReq}) \tag{3}$$

$$X_{Ragg} = \frac{1}{n+1} \cdot \text{imag}(Z_{LReq}) \tag{4}$$

Where the equivalent no load and locked rotor impedances are given by (5) and (6) respectively.  $i = 1, 2, \dots, N$

$$Z_{NLeq} = \frac{1}{\sum_{i=1}^N \frac{1}{Z_{NLi}}} \tag{5}$$

$$Z_{LReq} = \frac{1}{\sum_{i=1}^N \frac{1}{Z_{LRi}}} \tag{6}$$

The ratio of leakage inductances can be obtained by:

$$n = \frac{X_{sagg}}{X_{Ragg}} \tag{7}$$

The aggregate moment of inertia and mechanical power output were obtained using (8) and (9) respectively.

$$J_{Agg} = \sum_{i=1}^N J_i \cdot \left( \frac{\omega_{ri}}{\omega_{rAgg}} \right)^2 \tag{8}$$

Where

$\omega_{ri}$  = the individual motors rotor angular speed

$\omega_{rAgg}$  = the aggregate motors rotor angular speed

$$P_{Agg} = \sum_{i=1}^N P_i \tag{9}$$

The open circuit time constant and inertia are often used in the classification of motors. The loads were grouped together using the criterion developed in [14] and discussed in [15] which can be expressed as:

$$G = H \times a \times b \tag{10}$$

Where  $G$  is the homogeneity constant expressed by constants  $H$ ,  $a$  and  $b$  obtained by:

$$H = \frac{K.E}{S} \tag{11}$$

$$a = \frac{x_m}{r_r} \tag{12}$$

$$b = \frac{x_s + x_r}{r_s + r_r} \tag{13}$$

The  $x_s, x_r, r_s, r_r, x_m, S$  and  $K.E$  are the stator reactance, rotor reactance, stator resistance, rotor resistance, magnetizing reactance, MVA rating and kinetic energy respectively.

The group will be homogeneous if:

$$1 \leq \frac{G_{max}}{G_{min}} \leq 2.5 \tag{14}$$

The data for the electrical ship loads at the Mombasa port in Kenya was obtained from [6]. Given in Appendix A Table 3 are computed constants (11), (12) and (13)

governing the homogeneity constant (10) for the electrical ship loads. The ship motor loads were grouped into four using (14).

According to the power bill report in February 2016, the peak power demand at the Mombasa port in Kenya is estimated to range from 0.17MW to 12MW for vessels as small as container ships to large vessels like oil tankers and cruise ships. A detailed analysis of the off-shore load on the Mombasa port has been done. The total off-shore load is approximately 22MW. From the analysis, the Mombasa port has 22 berthing points with 9 berths for cargo ships, 9 for container ships, 2 for roll-on roll-off (Ro-Ro) [6]. Aggregation of the grouped motor loads was done using the no-load and locked rotor approach proposed in [16]. The parameters for the aggregated loads are in Table 1.

**Table 1.** Aggregate Parameters for the Ship Loads

parameters	Group 1	Group 2	Group 3
P (kW)	216.2	367.5	370
Rs, Ω	0.0794	0.0323	0.0550
Xs, Ω	0.0228	0.0098	0.0091
Rr, Ω	0.0237	0.0198	0.0450
Xr, Ω	0.0228	0.0146	0.0210
Xm, Ω	1.5759	0.5693	1.4610
J (kgm <sup>2</sup> )	9.4660	24.1918	11.0984
N (rpm)	1487	1483	1487

## II.II Network Model

The parameters for the developed model were obtained from [6] where the coastal power network description is given in detail and this network is part of the Kenya national power grid. The model is composed of 15 buses, 17 transmission lines, 4 generators and 12 loads. The network is connected to a 132kV supply point from the control center at Juja road in Nairobi. There is an additional supply transmission line of 220V from the Kiambere power station. The generators are located at four generating points: Rabai, Kipevu I, Kipevu II and Kipevu III and each with an installed capacity of 90MW, 75MW, 74MW and 120MW respectively.

The model was developed using the PSAT toolbox in the MATLAB software as detailed in Appendix B Fig. 9 with the additional off-shore ship load and generators. It was assumed that all the three aggregate motors are connected to the same bus. The ratings of the aggregate motors were also assumed to be 3MVA at a source voltage of 0.415kV. The aggregate resistance and reactance parameters were referred to the base values of the entire system (132kV and 100MVA) using the per unit system.

$$Z_{p.u., new} = Z_{p.u., old} \left( \frac{kV^2_{base, old}}{S_{base, old}} \right) \left( \frac{S_{base, new}}{kV^2_{base, new}} \right) \quad (15)$$

In the developed dynamic model, the bus voltages are not fixed. To control the voltages, generators with ratings equivalent to the power produced at the four generating points (Rabai, Kipevu I, II & III) were connected at the respective buses Fig. 9.

Multiple TDS were done before and after the inclusion of the corrective measures (AVR) with the system under a three-phase fault on the bus with the off-shore loads. A comparative analysis was done before and after increasing the ship load to assess the effectiveness of the STATCOM device.

### II.III STATCOM

STATCOM is a second-generation Voltage Source Converter (VSC) FACTS device that is non-thyristor based. It is shunt connected to the power system. This device can control the specific parameters of a power system such as voltage by injecting or absorbing reactive power at the point of common coupling by varying its output [17]. The exchange of the reactive power occurs between the STATCOM and alternating current (AC) system. Fig. 2 shows the configuration of the STATCOM [18].

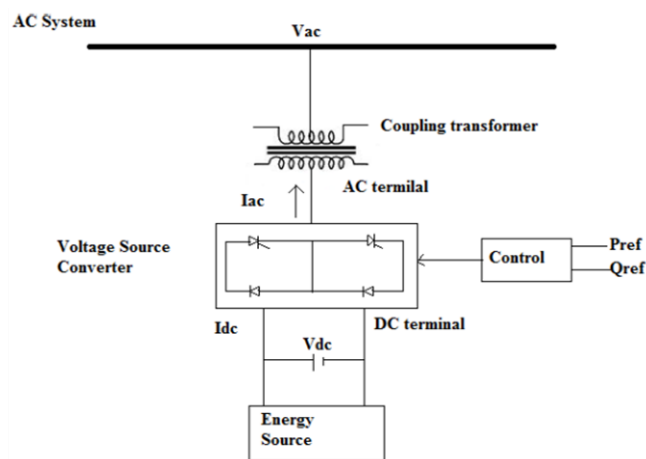


**Fig. 2.** STATCOM Configuration

The reactive power ( $Q$ ) is injected into the AC system when its voltage magnitude is low and  $Q$  is absorbed when the system voltage magnitude is high. The voltage source converter (VSC) seen in Fig. 2 feeds the reactive power into the system. The STATCOM control system operates such that it varies the VSC output voltage magnitude and phase shift controlling the reactive power exchange at the coupling point [18][19].

A power flow analysis was done to obtain the voltage magnitudes of the system during a three-phase fault. The STATCOM was placed on the KPA bus which was found to have the lowest voltage magnitude.

#### **II.IV Dynamic voltage stability Analysis**

Voltage stability is greatly influenced by the dynamic behavior of a power system which is basically a large dynamic system. By definition, voltage stability is the ability of a power system to maintain acceptable voltages at all buses in the system under normal operating conditions and after being subjected to a disturbance. Voltage stability analysis is done to help determine the systems loading ability and how close or far it is from the voltage collapse point. It is classified into large and small disturbance voltage stability. Small disturbance voltage stability is concerned with the power system's ability to control voltages following a small interruption such as change in load, whereas, large disturbance voltage stability has to do with the ability of the system to maintain acceptable voltage following large perturbations such as system faults, loss of load or generation [12][20][21].

The analysis of voltage stability can be done either dynamically or statically. Dynamic voltage stability analysis focuses on how the loads in the system change and how these changes affect the voltage magnitudes of the buses where loads are connected. The dynamic nature of the loads is put into consideration. Time domain simulations (TDS) and other analytical tools are used in this analysis [22]. The mathematical expression of dynamic analysis is made up of a set of algebraic equations and first order differential equations. It is given as [20] and [21] :

$$x = f(x, y) \quad (15)$$

$$0 = g(x, y) \quad (16)$$

Where  $x$  is the state vector of the system and  $y$  is the vector containing the bus voltages.

To provide a source of disturbance to the system, a three-phase fault was introduced on the bus with the off-shore load. The bus was selected because voltage stability analysis focuses on the local load and in this study, the off-shore load is the area of focus and it had the lowest voltage magnitude. The fault was set to occur at 2.00 seconds and cleared at 2.25 seconds. The simulations were conducted and observation made on the dynamic voltage stability responses of the buses affected by the fault under three cases.

Case 1: TDS is carried out with three-phase fault without the AVRs

Case 2: TDS is carried out with three-phase fault with the AVRs

Case 3: TDS is carried out with three-phase fault with the AVR and STATCOM connected to the power network.

The dynamic voltage stability enhancement responses from the third case TDS were obtained and used to do a comparative analysis alongside the results of case 1 and 2 without and with increased ship load.

### III. RESULTS

#### III.I Analysis before increasing the ship load

The results for the TDS without the AVRs and STATCOM, with AVR and, with AVRs and STATCOM are as presented in Fig. 3 to Fig. 5. From the figures, it is observed that the occurrence of a fault led to a voltage dip at buses 2 (KPA), 4 (Kipevu I&III), 5 (Kipevu II) and 18 (off-shore) in the network.

During post fault, it is noted that the voltage of the affected buses starts to drop from its nominal operating point on case 1 (without AVRs and STATCOM). The system is not able to maintain a steady state operating point as before the introduction of the disturbance. The occurrence of a fault and with the off-shore load led to the fluctuations of the system voltage leading to a voltage collapse after 17.35 seconds.

The AVRs were connected to the generators and a TDS was done to check their effectiveness on the system's voltage response. The following observations were made as shown in Fig. 3 to Fig. 5. It is noted that with the AVRs, in the presence of the ship load and a three-phase fault, the system is able to go back to its steady operating point after fault clearing. Also observed is that the TDS ran to 100% without the system experiencing voltage collapse as compared to when the system had no AVRs.

A dynamic model for the STATCOM FACTs device was developed and used to assess the impact of the device on the power network during a disturbance. The STATCOM was placed on the KPA bus of the system and a TDS was carried out and the results are as presented in Fig. 3 to Fig. 5. From the plots, it is observed that the STATCOM does not have a significant impact on the system. The AVRs are able to meet the reactive power demands of the induction motors of the ship load adequately.

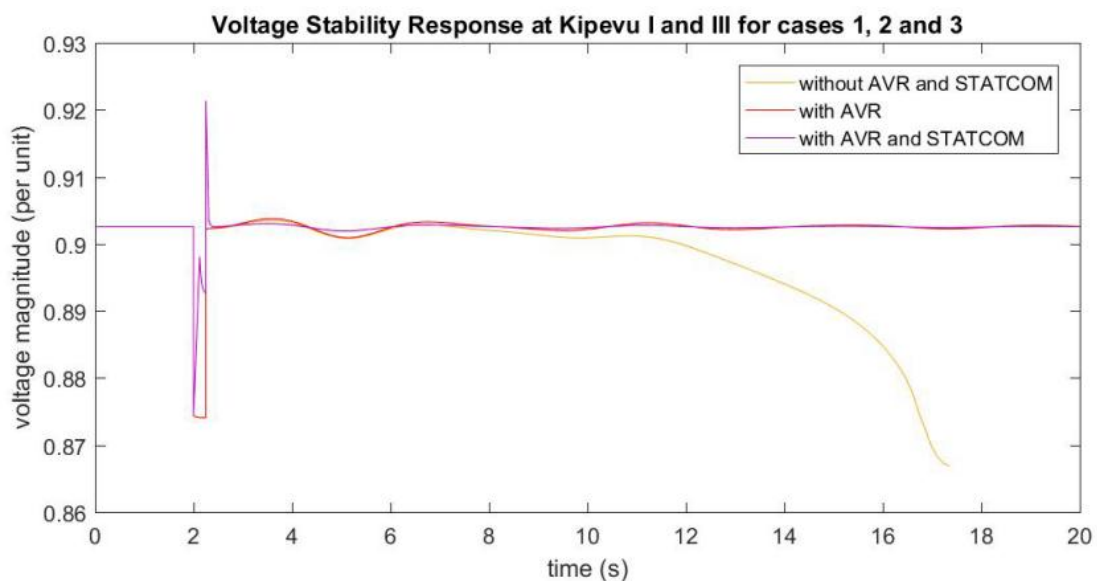
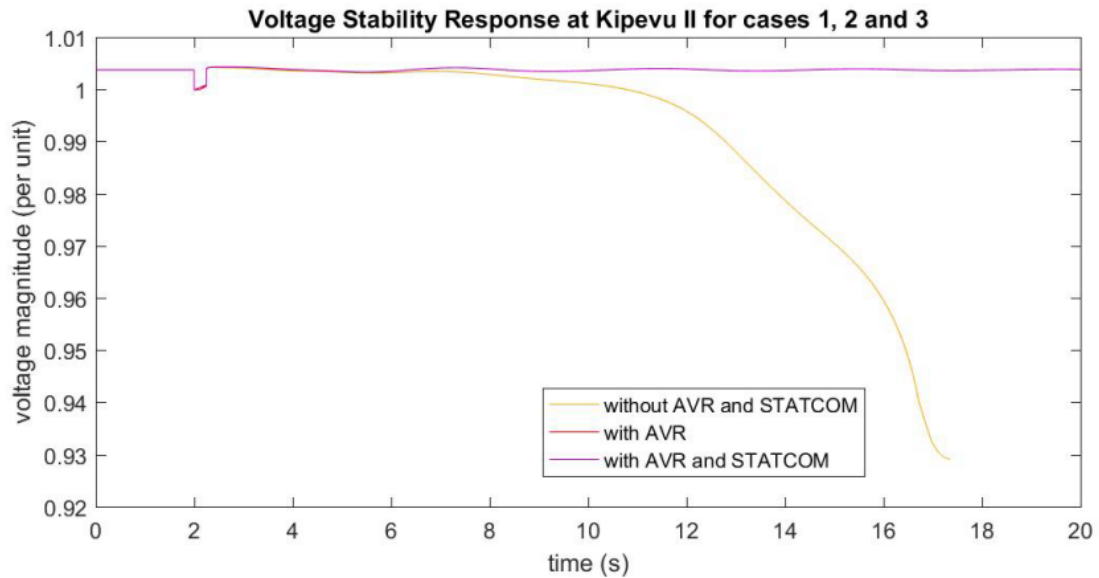
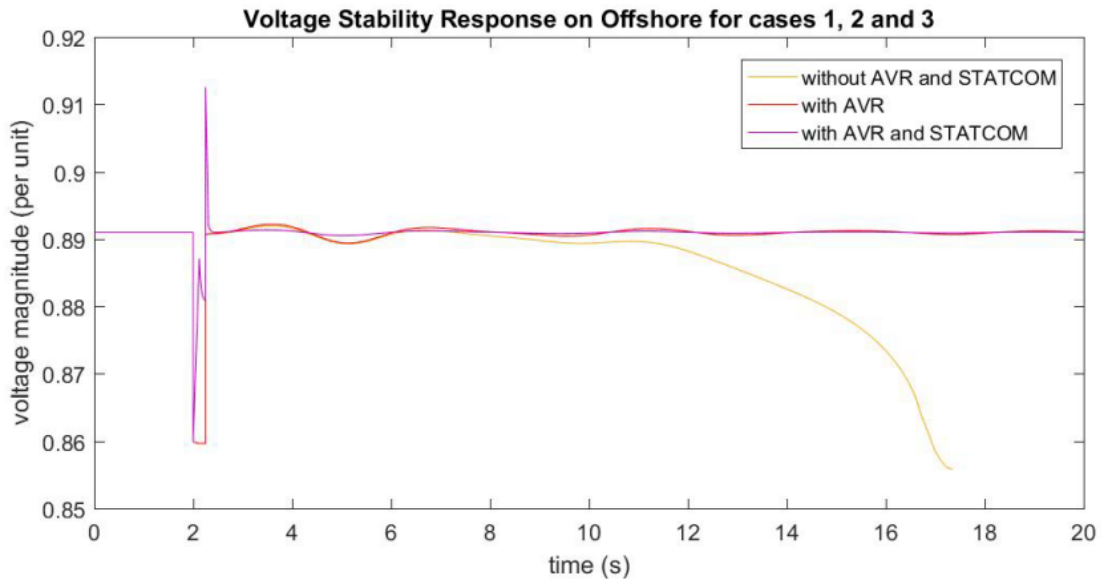


Fig. 3. Voltage stability response on Kipevu I&III bus during and post fault



**Fig. 4.** Voltage stability response on Kipevu II bus during and post fault



**Fig. 5.** Voltage stability response on Off-shore bus during and post fault

### III.II Analysis after increasing the ship load

The off-shore load was increased to twice the initial capacity and the following observations were made as shown in Fig. 6 to Fig. 8. Table 2 shows the ship loads before and after the increase. Without AVRs and STATCOM, the voltage of the affected buses drops from its nominal operating point resulting to a voltage collapse after 2.0 seconds.

It is also observed that addition of the AVRs to the system does not improve the condition of the network. The system's voltage response fluctuates and drops leading to a voltage collapse after 4.22 seconds. The AVRs are not able to provide enough reactive power compensation for the extra ship load when a 3-phase fault occurs in the system.

On adding the STATCOM, it is noted that the system was able to regain stability after about 2.39 seconds as seen in Fig. 8.

**Table 2.** Ship motor loads

Parameter	Before increased load			After increased load		
	Group 1	Group 2	Group 3	Group 1	Group 2	Group 3
Real power, P (pu)	0.042	0.071	0.078	0.084	0.142	0.156
Reactive power, Q (pu)	0.576	0.574	0.581	1.152	1.148	1.162

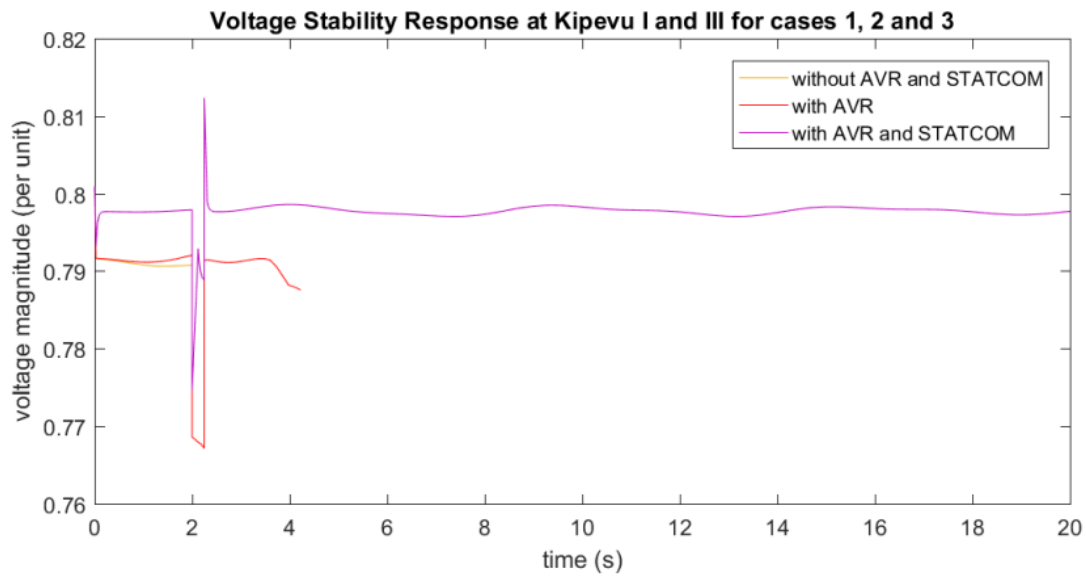


**Fig. 6.** Voltage stability response on Kipevu I&III bus during and post fault

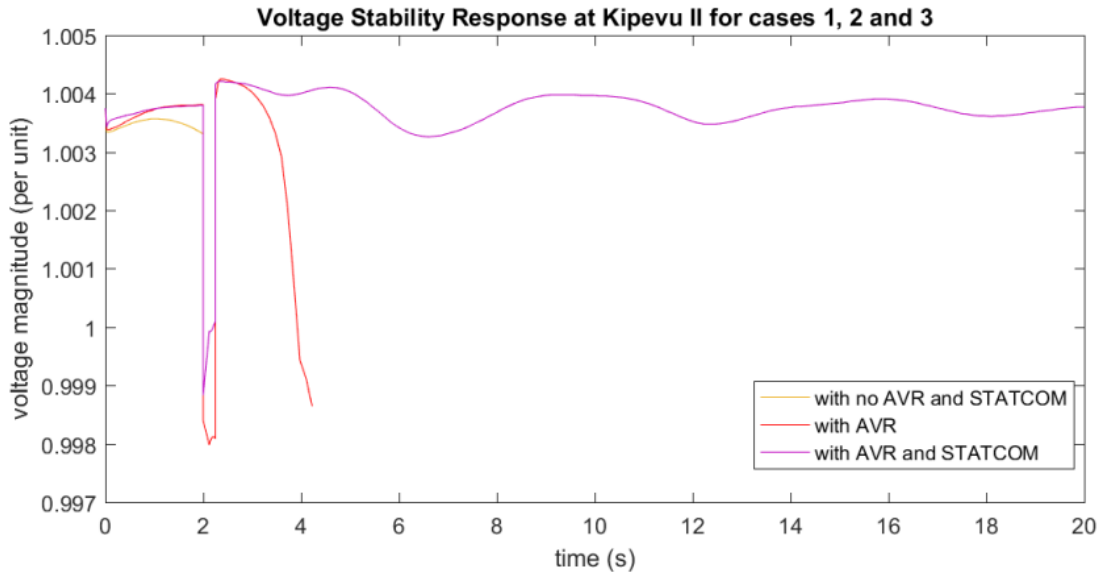


**Fig. 7.** Voltage stability response on Kipevu II bus during and post fault

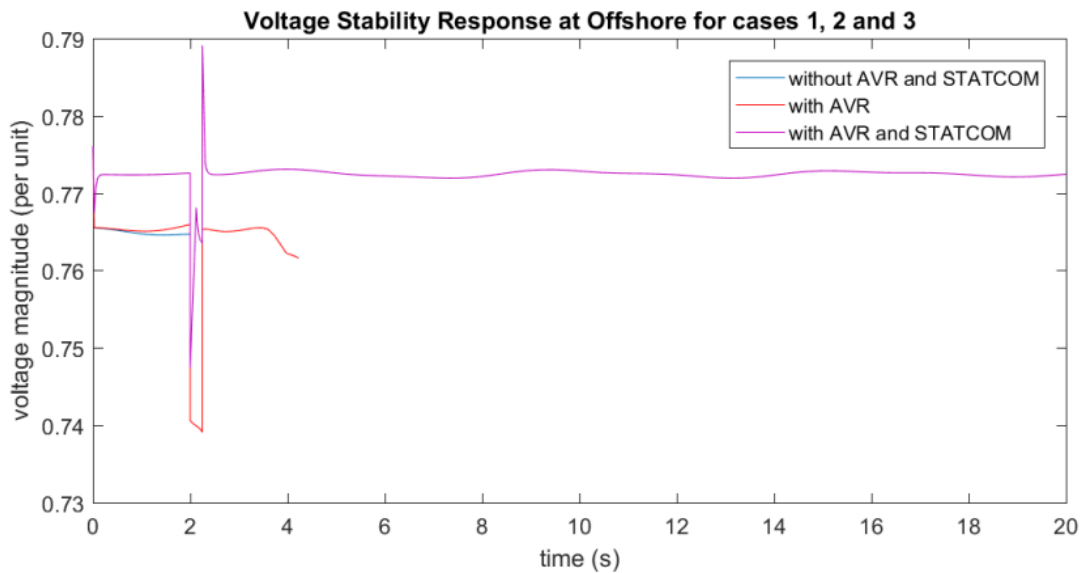


**Fig. 8.** Voltage stability response on Off-shore bus during and post fault

#### IV. CONCLUSION

The ship loads were aggregated and connected to the Kenyan Coastal power network. A dynamic model connected with the off-shore load was developed. A 3-phase fault was introduced at the off-shore bus to provide a disturbance to the system. The

dynamic voltage stability analysis was done under three condition to assess the systems response with and without the increased ship load.

Before increasing the ship load, it was observed that without the AVRs and STATCOM, the system's voltage response fluctuates during the post fault leading to voltage collapse. The study reveals that addition of the AVRs to the network prevented voltage collapse and the system regains its steady state operating condition. On adding the STATCOM it was noted that its impact is not significant as the AVR are able to provide enough reactive power compensation to the motor ship loads during the three-phase fault.

After increasing the ship load, the system experienced voltage collapse on both case 1 (no AVR and STATCOM) and case 2 (with AVR). The study shows that by connecting the STATCOM to the network, the system regains a steady state operating condition. The STATCOM was able to provide enough reactive power compensation for the motor ship loads during the transient period.

## REFERENCES

- [1] E. A. Sciberras, B. Zahawi, and D. J. Atkinson, "Electrical characteristics of cold ironing energy supply for berthed ships," *Transp. Res. Part D Transp. Environ.*, vol. 39, no. December, pp. 31–43, 2015.
- [2] D. Radu, R. Jeannot, M. Megdiche, and J. P. Sorrel, "Shore connection applications : Main challenges," *Schneider Electr.*, no. July, pp. 1–36, 2013.
- [3] E. A. Sciberras, B. Zahawi, D. J. Atkinson, A. Juandó, and A. Sarasquete, "Cold ironing and onshore generation for airborne emission reductions in ports," *Proc. Inst. Mech. Eng. Part M J. Eng. Marit. Environ.*, vol. 230, no. 1, pp. 67–82, 2016.
- [4] T. Borkowski and D. Tarnapowicz, "' Shore to ship ' system – An alternative electric power supply in port," *J. KONES Powertrain Transp.*, vol. 19, no. 3, pp. 49–58, 2012.
- [5] M. Ion, M. Megdiche, S. Bacha, and D. Radu, "Transient analyses of a shore-to-ship connection system," in *International Conference on Power Systems Transients (IPST 2013)*, 2013.
- [6] C. N. Karue, D. K. Murage, and C. M. Muriithi, "Shore to ship power for Mombasa port possibilities and challenges," no. May, pp. 4–6, 2016.
- [7] C. N. Karue, D. K. Murage, and C. M. Muriithi, "Modelling and loading limits for Kenya coast power network using continuation power flow," *Int. J. Energy Power Eng.*, vol. 5, no. 6, pp. 182–188, 2016.
- [8] C. N. Karue, D. K. Murage, and C. M. Muriithi, "On-Shore power supply stability analysis on 132 kV Mombasa power distribution network," in *Proceedings of the Sustainable Research and Innovation Conference*, 2017, no. May, pp. 30–36.
- [9] K. R. Padiyar, *FACTS controllers in power transmission and distribution*. New Delhi: New Age International Publishers, 2007.
- [10] J. Zhou, J. Zhang, Y. Yang, and Y. Ju, "Dynamic aggregation method of induction motors based on coherent characteristics," pp. 441–442, 2012.

- [11] P. Pillay, "A model for induction motor aggregation for power system studies," vol. 42, pp. 225–228, 1997.
- [12] S. B. Bhaladhare, A. S. Telang, and P. P. Bedekar, "P-V , Q-V Curve – A novel approach for voltage stability analysis," *Natl. Conf. Innov. Paradig. Eng. Technol.*, pp. 31–35, 2013.
- [13] T. Kataoka, H. Uchida, S. Nishikata, T. Kai, and T. Funabashi, "A Method for aggregation of a group of induction motor loads," in *PowerCon 2000 - 2000 International Conference on Power System Technology, Proceedings*, 2000, vol. 3, pp. 1683–1688.
- [14] M. Akbaba and S. Q. Fakhro, "New model for single-unit representation of induction motor loads, including skin effect, for power system transient stability studies," *IEE Proc. B Electr. Power Appl.*, vol. 139, no. 6, p. 521, 1992.
- [15] J. M. Kinyua, C. M. Mureithi, D. K. Murage, and L. Obiri, "Comparison of aggregation methods of induction motor models for transient stability load modeling."
- [16] A. Karakas, F. Li, and S. Adhikari, "Aggregation of multiple induction motors using MATLAB-based software package," in *2009 IEEE/PES Power Systems Conference and Exposition, PSCE 2009*, 2009, pp. 1–6.
- [17] R. M. Mathur and R. K. Varma, *Thyristor based FACTS controllers for electrical transmission systems*. New York: JOHN WILEY & SONS, INC., 2002.
- [18] A. Vijayan and S. Padma, "Maintaining Voltage Stability in Power System using FACTS Devices," *Int. J. Eng. Sci. Invent.*, vol. 2, no. 2, pp. 20–25, 2013.
- [19] H. Marefatjou and I. Soltani, "Optimal Placement of STATCOM to Voltage Stability Improvement and Reduce Power Losses by Using QPSO Algorithm," *J. Sci. Eng.*, vol. 2, no. 2, pp. 105–119, 2013.
- [20] P. Kundur, *Power system stability and control*. New York: McGraw Hill, 1994.
- [21] L. J. Cai and I. Erlich, "Dynamic voltage stability analysis in multi-machine power systems," *15th Power Syst. Comput. Conf. ...*, no. August, pp. 22–26, 2004.
- [22] S. N. Njoroge, C. M. Muriithi, and L. M. Ngoo, "Dynamic voltage stability analysis of the Kenya power system using VCPI stability index and artificial neural networks," vol. 3, no. 7, pp. 23–30, 2014.

**APPENDIX A**

Table 3. Homogeneity Constants for The Electrical Ship Loads

Type of load	Quantity	Total kW	Total HP	H (s)	a	b	poles	G
Cooling sea w/pump	1	28.9	39	0.444	78.06	0.4133	4	14.32
C/Fresh w/pump	1	12.4	17	0.454	130.94	0.3013	4	17.91
M/E lube oil	1	69.9	94	0.364	28.94	0.4651	4	4.899
Exhaust valve pump	1	4.4	6	0.426	34.01	0.5783	4	8.379
Fuel oil boiled motor	2	5.6	8	0.458	36.37	0.5571	4	9.356
Fuel oil circ. Pump	1	6.3	8	0.407	36.67	0.5571	4	8.315
Fuel oil trans. pump	1	8.5	11	0.418	44.38	0.5055	4	9.377
G/E sea w/pump	1	16.7	22	0.431	119.18	0.3154	4	16.200
G/E D. O supp. Pump	1	3.8	5	0.416	33.06	0.5869	4	8.070
Ballast/pump	1	39.8	53	0.427	60.93	0.5179	4	13.470
Fire and GS	1	39.8	53	0.427	60.93	0.5179	4	13.470
Fire, Ballast	1	86.4	116	0.370	26.14	0.4324	4	4.180
Air comp. Engine	2	95.6	128	0.376	26.38	0.4412	4	4.376
R/vent	2	115.6	155	0.474	32.33	0.4615	4	7.072
A/C plant	1	28.9	39	0.444	78.06	0.4133	4	14.320
A/C fan	1	16.7	22	0.431	119.18	0.3154	4	16.200
Cooking range	4	100	134					
Plant/comp	1	4.4	6	0.426	34.01	0.5783	4	8.379
Cargo cranes	2	370	497	0.140	32.33	0.3000	4	1.435
Lighting (all)	1	22.86	31					
Refer containers	150	5220	7005	0.00325	60.93	0.6170		0.122
Total	177	6297	8449					

APPENDIX B

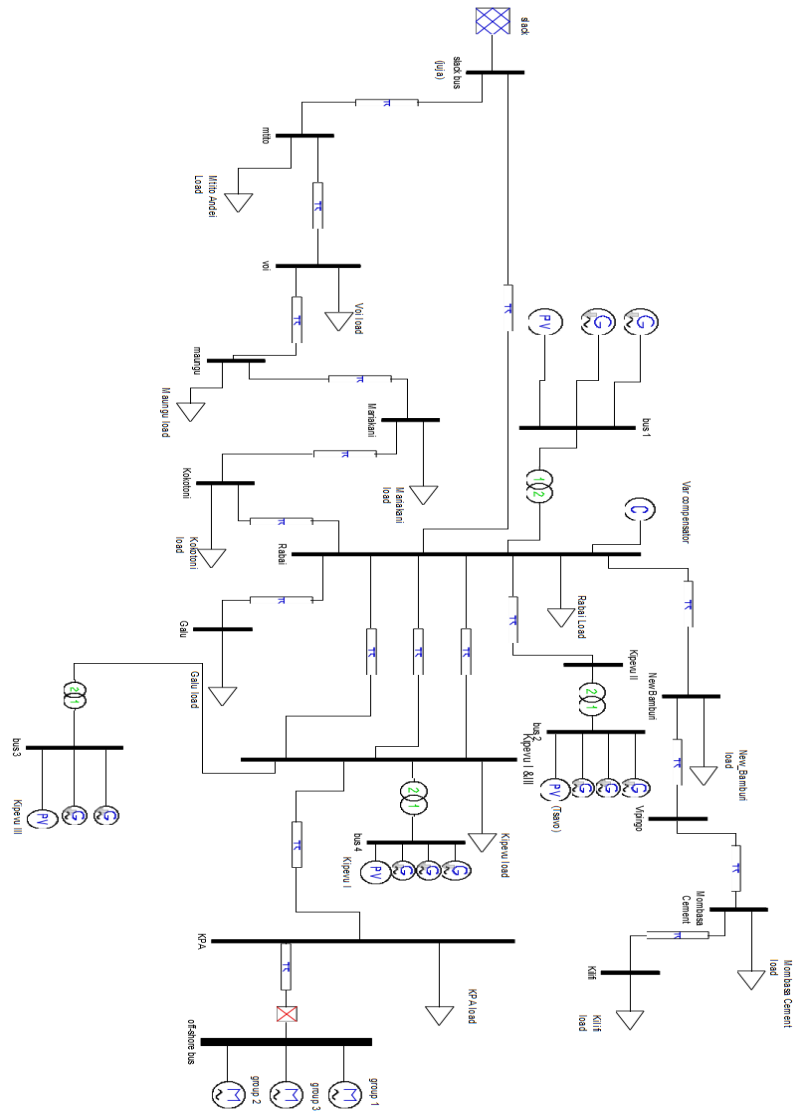


Fig. 9. Network model of Coastal network using Matlab/PSAT